STRUCTURAL ASPECTS OF METEOR CRATER AND THEIR EFFECT ON CRATERING. M. H. Poelchau[1], T. Kenkmann[1], D. A. Kring[2], [1]Museum für Naturkunde, Invalidenstr. 43, 10115 Berlin, Germany, [2]Center for Advanced Space Studies, LPI, Houston, Texas. (michael.poelchau@museum.hu-berlin.de)

Introduction: Meteor Crater, located in Arizona, USA, shows obvious morphological deviations from a circular crater shape. Its square shape has been interpreted to be a consequence of a regional joint system that runs diagonally to the square [1,2; Fig. 1a].

Meteor Crater was structurally examined to investigate the effects of target anisotropies and obliquity on the cratering process. Here we present structural data and first qualitative models are shown to explain the phenomena observed in the field. In particular, detailed measurements of bedding strike and dip were collected around the entire crater rim together with GPS data.

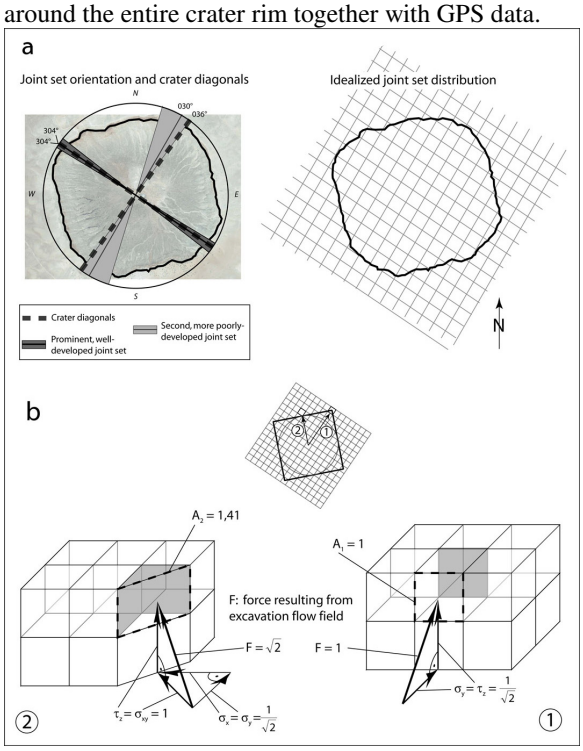

Fig. 1: A simplified model correlating joint sets (data from [2]) and bedding planes with crater formation.

Joints: Field data from [2] shows a striking correlation between crater diagonals and the orientation of joint sets. These joints have a spacing ranging between 0.5-10 m and have subdivided the target into small, square-shaped units (Fig. 1a).

Tear faults: Joint sets form structurally weak zones along which tear faults have propagated during crater formation. The major tear faults are oriented subparallel to these joints. Tear faults are localized expressions of differential movement between blocks that occurred during rim uplift. The main component of movement is vertical, along with a rotational component or "scissors type of displacement" [1] that tips the blocks outwards. The highest uplift of strata (e.g. ~45 m displacement in the SE) occurs along these faults. This has led to an asymmetric structure of the crater rim in which the entire S and N sides of the rim appear as lower, downfaulted blocks relative to the corners, as shown in the bedding data.

Bedding data: For the display in a stereo plot (Fig. 2) the bedding dataset was split into crater corners and sides. The data shows four clusters of poles reflecting the four sides of the crater wall. The N and S sides have more concentrated poles, compared to the more scattered E and W sides. This indicates rotation in the E and W sides. The S side dips more gently on average than the E and W sides, while the N side has the steepest dip. The SE and SW corners show strong scattering and rotation. The data is more complex than a simple, square-shaped deviation. The factors that we believe control this complex, non-radial behavior are discussed below.

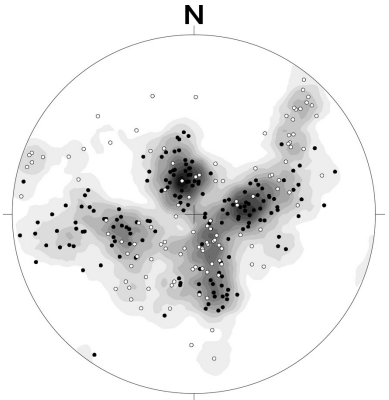

Fig. 2: Stereo plot of 298 bedding points. White: corners; black: sides of crater wall.

Uplift: The elevation of both the lower Coconino-Kaibab (CK) contact and the Kaibab-Moenkopi (KM) contact were measured for a better control of differential uplift in the crater wall. Based on geological and topographical maps, average height of the CK contact is ~1645 m within and 1590 m outside the crater. Maximum elevation of the CK contact is higher in the corners of the crater (>1670 m) than along the sides (~1640 m), resulting in an uplift from pre-impact CK elevation of ~50 m on the sides to a maximum of 80 m in the corners (the contact is not exposed in the NW

corner). This differential uplift between corners and sides is a result of major tear faults located in all four corners of the crater.

GPS data of the KM contact situated in the upper crater rim principally correspond to the CK contact and reveal a correlation between the distance of beds from the crater center and their elevation. Although the correlation is rough, there is a definite trend for the KM contact to be in a higher position the further away it is from the crater center, that is the more they are located in the corners of the quadrangular crater. Undulations in the height of the KM contact are caused by injections of coherent fault blocks into the upper crater wall, which we denote as "thrust wedges".

Thrust wedges: In addition to the two directions of weakness caused by joint sets and used by tear faults, a third zone of weakness can be found in the horizontal layering of rock beds. Thrust wedges use this zone of weakness and can be found in several areas of the crater wall [1]. These wedges have an effect on uplift. Where they occur, the top Kaibab and Moenkopi units are arched up and form anticlinal features (Fig. 3b).

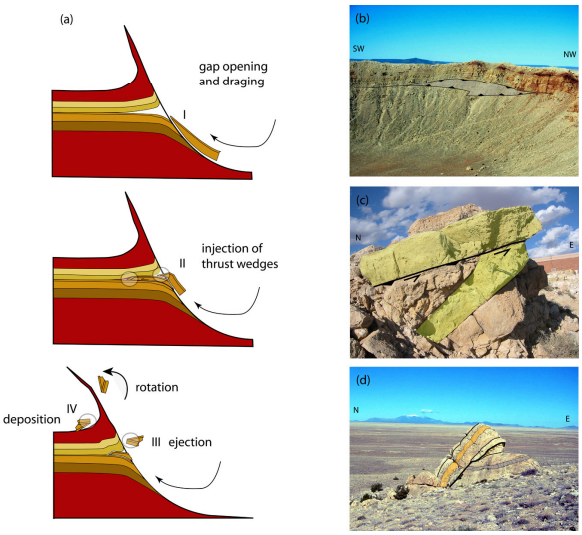

Fig. 3: Field observations and a model for the formation of "thrust wedges".

Model 1: Based on field observations (Fig. 3b-d) we propose a model for the formation of thrust wedges. We assume that during crater excavation, outward and upward directed excavation flow opens small gaps along horizontal areas of weakness in upper stratigraphic units (Fig. 3a-I), which are used by the tips of incipient thrust wedges (II). Further thrusting of these wedges into the gaps creates additional uplift, raising overlying units to a higher elevation than neighboring beds. In the ejecta, meter sized units of Kaibab were found with obliquely terminating bedding planes (Fig. 3c,d). We interpret these as thrust ramps from the initial phase of thrust wedge formation, which were then excavated (III) and deposited as ejecta (IV).

Model 2: In an attempt to understand the mechanical aspects behind the formation of the square shape of Meteor Crater, we suggest a simplified, qualitative model that compares surface stress to the excavation force exerted on rock units (Fig. 1). In this model we divide the target rock into discrete cubes, based on the two joint sets plus horizontal layering planes. During cratering, the excavation flow field that ejects rock is directed outward and upward in the upper part of the crater. For simplification, we assume the flow field is oriented radially from the crater center and upwards at 45° (Fig. 1b). We can observe two situations in this model, one where the flow field is directed parallel to one of the joint sets (Fig. 1b-1), and one which is directed at a 45° angle to both joint sets (Fig 1b-2). The flow field exerts a force on the cube, which is proportional to the exposed surface of the cube, thus resulting in a force that is $\sqrt{2}$ times stronger in 2. This force can be split into horizontal and vertical components that correspond to normal stress (σ_x, σ_y) and shear stress (τ_z), respectively. Vector addition (Fig. 1b) shows that the ratio of normal stress to shear stress in situation 1 is $\sigma_y : \tau_z = 1$. In situation 2 the ratio is $(\sigma_x + \sigma_y) : \tau_z = \sqrt{2}$, due to the larger surface area exposed to the flow field and the circumstance that shear stress is exerted on two surfaces of the cube (marked in gray in Fig 1b), as opposed to one surface in situation 1. As less shear stress is resolved in situation 1 excavation should progress faster and further, and the initial circular crater shape should start getting corners, resulting in the final square shape seen in Meteor Crater. It should be noted that target anisotropies such as joints become important mainly in the final stages of crater excavation, when the stresses induced by the excavation flow are in the order of the strength of the target material.

Conclusions: This model provides a basic understanding of how joint sets and weaknesses in bedding planes affect the late stages of the cratering process. Questions remain on how the more detailed, complex structures in the crater rim were formed. Certain aspects, like the somewhat counterintuitive correlation between radial distance and uplift in Meteor Crater still need to be contemplated.

Acknowledgements: We would like to thank the DFG for funding this project (KE 732-11/1).

References: [1] Shoemaker E. M. (1960) *Structure of the Earth's Crust and Deformation of Rocks. Rept. 18*, 418-434. [2] Roddy D. J. (1978) *Proc. Lunar Planet. Sci. Conf. 9th*, 3891-3930.